

Peculiarities of β -Pinene Autoxidation

Ulrich Neuenschwander, Emanuel Meier, and Ive Hermans^{*[a]}

The thermal oxidation of the renewable olefin β -pinene with molecular oxygen was experimentally and computationally investigated. Peroxyl radicals abstract weakly bonded allylic hydrogen atoms from the substrate, yielding allylic hydroperoxides (i.e., myrtenyl and pinocarvyl hydroperoxide). In addition, peroxyl radicals add to the C=C bond of the substrate to form an epoxide. It was found that a relatively high peroxyl radical concentration, together with the high rate of peroxyl cross-reactions, make radical–radical reactions surprisingly important

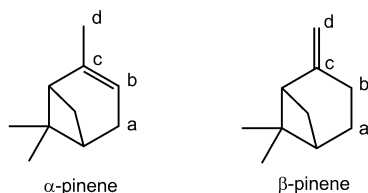
for this particular substrate. Approximately 60% of these peroxyl cross-reactions lead to termination (radical destruction), keeping a radical chain length of approximately 4 at 10% conversion. Numerical simulation of the reaction—based on the proposed reaction mechanism and known or predicted rate constants—demonstrate the importance of peroxyl cross-reactions for the formation of alkoxy radicals, which are the precursor of alcohol and ketone products.

Introduction

α -/ β -Pinene as renewable resources

α - and β -pinene (Scheme 1) are two chief constituents of turpentine oil, which can be obtained by the distillation of pine tree resins or as a by-product of the kraft pulping process.^[1]

In the kraft or sulfate process, wood chips are heated to 150–180 °C in an aqueous digestion mix (NaOH, Na₂S, Na₂CO₃ and small quantities of Na₂SO₄, Na₂SO₃ and Na₂S₂O₃) in large pressure vessels at 7–13 bar for several hours.^[1] Crude sulfate turpentine is condensed from the waste gas from the digester and is separated from the water. It still contains 5–15 wt% sulfur compounds (e.g., MeSH, Me₂S). These can be oxidised with NaOCl solution at about 60 °C to give the less volatile sulfonic acids, sulfoxides or sulfones, which can be effectively separated by washing with water or by distillation. The yield of refined sulfate turpentine is approximately 10 kg per ton of pulp for pine trees. The location and date of the wood harvest, as well as the length of the storage period before processing, all affect the yield and the composition of the product. Typical American turpentine oil contains 60% α - and 30% β -pinene. The world production of sulfate turpentine reached 6 × 10⁵ tons per year in 2008,^[2] making up two-thirds of the total turpentine production. Production has more than doubled since 1990. Moreover, if bio-refineries^[3] make it to the industrial market, a significant increase in turpentine availability can be anticipated.



Scheme 1. Structure of the two regional isomers α - and β -pinene. The four different oxidation sites are denoted a–d.

Terpenic isomers are therefore cheaply available renewable resources that can be used for a wide range of applications. α -Pinene is, for instance, converted into α -pinene oxide, which is a precursor for all synthetic sandalwood fragrances.^[4] β -Pinene is a substrate for the synthesis of insecticides,^[5] menthol and fragrance products such as camphor. Both isomers, as well as their oxidised derivatives, are desired in perfumery due to their woody pine odour.^[6] α -Pinene can be found in both enantiomeric forms in different turpentine types. β -Pinene from turpentine sources is usually found in enantiopure (–) form (enantiomeric excess (*ee*) > 95%).^[7] The other enantiomer, (+)- β -pinene, prevails in citrus fruit oil.^[8]

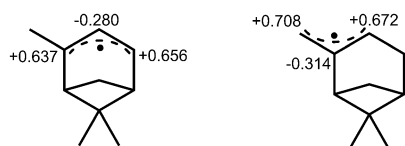
A publication by Widmark and Blohm in 1957 reported the autoxidation rates of different monoterpenes (e.g., Δ^3 -carene, α -pinene, β -pinene and (+)-limonene) at room temperature in air, but not the product distribution.^[9] Recently, we reported the mechanism of the oxyfunctionalisation of α -pinene.^[10,11]

α -Pinene autoxidation

The autoxidation of α -pinene was previously studied and found to be propagated by four different peroxyl radicals, namely, verbenyl ($R_{(a)}OO^*$), pinocarvyl ($R_{(b)}OO^*$), pinenyl ($R_{(c)}OO^*$) and myrtenyl peroxyl radical ($R_{(d)}OO^*$).^[10] These radicals abstract weakly bonded α -hydrogen atoms in the substrate, yielding the corresponding hydroperoxide and a resonance-stabilised alkyl radical. Hydrogen abstraction can occur both at the a and

[a] U. Neuenschwander, E. Meier, Prof. Dr. I. Hermans
Department of Chemistry and Applied Biosciences
ETH Zurich
Wolfgang-Pauli-Strasse 10, 8093 Zurich (Switzerland)
E-mail: ive.hermans@chem.ethz.ch
Homepage: <http://www.hermans.ethz.ch>

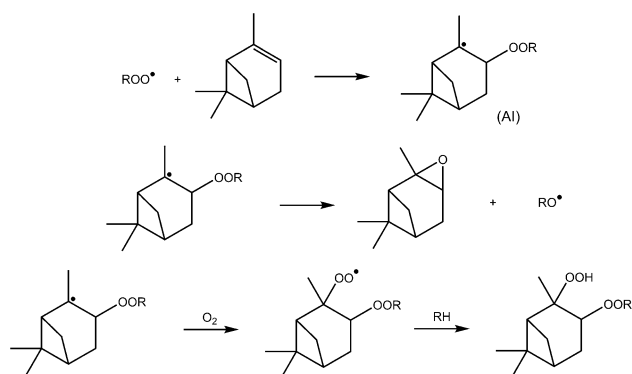
Supporting Information for this article is available on the WWW under <http://dx.doi.org/10.1002/cssc.201100266>.



Scheme 2. The two resonance-stabilised radicals formed upon abstraction of an H atom from the a (left) and d sites (right) of α -pinene and the Mulliken atomic spin densities of the most relevant atoms (UB3LYP/6-311 + G(df,pd)//UB3LYP/6-31G(d,p)-level).

d sites of α -pinene (Scheme 1); in both cases producing resonance-stabilised radicals (Scheme 2).

O_2 addition to these two allyl radicals generates the four $R_{(x)}OO^\bullet$ peroxy radicals. Competing with the hydrogen abstraction reaction is the addition of the peroxy radicals to the C=C double bond in the substrate (Scheme 3). The adduct intermediate (AI) can eliminate an alkoxy radical to form an epoxide or it can react with O_2 and ultimately yield a dialkyl peroxide (Scheme 3). At moderate oxygen pressures, epoxide formation is kinetically favoured.^[11]



Scheme 3. Addition of peroxy radicals to α -pinene; formation of pinene oxide.

The alkoxy radicals formed in the epoxidation step are converted into alcohols and ketones upon reaction with the substrate and O_2 , respectively. This explains the 1:1 ratio between the epoxide and the sum of alcohol and ketone up to 10% conversion. At higher conversions, more alcohol and ketone is formed than estimated from this 1:1 relation, due to the co-oxidation of the hydroperoxide, yielding additional alcohol and ketone upon abstraction of the α -hydrogen atom.

At increasing oxygen pressure, a significant decrease in epoxide selectivity was observed.^[11] Indeed, AI can be trapped with O_2 , preventing the formation of epoxide (Scheme 3). Associated with this is an increase in the reaction rate, due to enhanced initiation by the dialkyl peroxide produced. Also due to kinetic competition, ketone formation is favoured at higher O_2 pressures.^[11]

Although a lot of work has been carried out in the field of catalytic oxidation of β -pinene,^[12–15] a fundamental study on the radical-propagated autoxidation mechanism is lacking. The goal of this contribution is to verify if a similar mechanism is

responsible for the oxidation of β -pinene as that described for α -pinene.

Results and Discussion

Overall observations

β -Pinene oxidation was studied at 363 K (i.e., 90 °C) in a bubble column reactor under 1 bar of pure O_2 as described in the Experimental and Computational Section. Figure 1 shows the evolution of β -pinene conversion as a function of time:

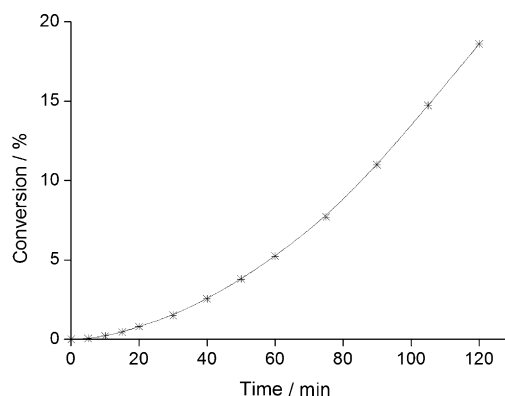


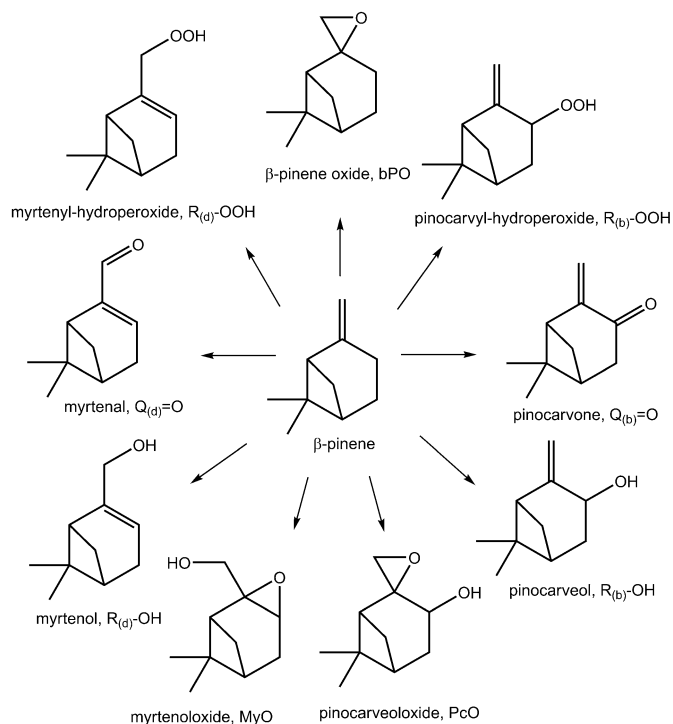
Figure 1. Time evolution of β -pinene conversion at 363 K.

after a short induction period of approximately 10 min, the conversion increases in an almost quadratic way. This is in stark contrast with the situation observed during cyclohexane oxidation,^[16] but similar to the behaviour observed during the autoxidation of ethylbenzene^[17] and α -pinene.^[10] The main reason for this difference in kinetic behaviour between the different substrates is the fact that ethylbenzene and α -pinene oxidation do not produce products that can accelerate the formation of radicals (chain initiation), in contrast to cyclohexanone during cyclohexane oxidation.^[18]

Scheme 4 summarises the main products of β -pinene autoxidation as identified by GC and GC–MS (see the Supporting Information).

Many of these products are valuable ingredients for the fine-chemical industry. Myrtenol, for instance, is used as a beverage preservative, a flavour ingredient, a fragrance,^[6] and can serve as an insect pheromone in insect traps by attracting pine bark beetles.^[5] Myrtenal is also used in the perfume industry, for instance, as a deodorant constituent, and can form an interesting ligand scaffold. Substituted or oxidised pinocarveol derivatives are promising fragrance compounds. Hydroperoxides can be reduced, for instance, with sodium sulphite, to increase the yield of the corresponding alcohol. β -Pinene oxide (bPO) can be rearranged into useful products such as perilla alcohol.^[19]

Figures 2 and 3 show the evolution of the most important products as a function of the sum of products, up to approximately 20% conversion. Similar to the situation with α -pinene oxidation, the product distribution is much less conversion de-



Scheme 4. Main products of β -pinene oxidation.

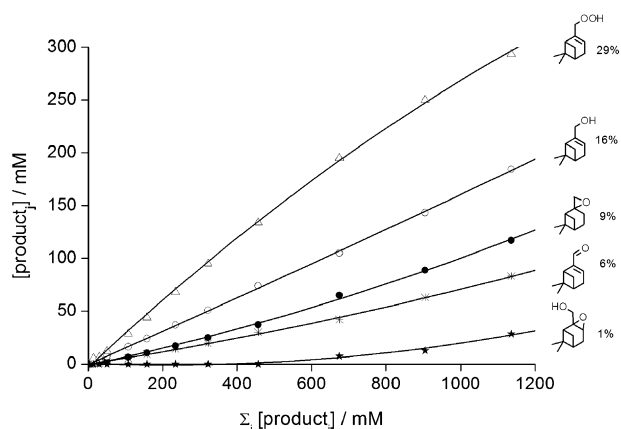


Figure 2. Evolution of the myrtenyl products (d-site oxidation products in Scheme 1) and bPO versus the sum of the products. The selectivity is reported at 10% conversion (i.e., $\Sigma[\text{product}] = 630 \text{ mM}$).

pendent than for cyclohexane autoxidation, meaning that consecutive over-oxidation is less important. The most remarkable over-oxidation products are pinocarveol oxide and myrtenol oxide, stemming from consecutive epoxidation of pinocarveol and myrtenol, respectively (the observed selectivities are zero up to 3% conversion).^[20]

An interesting observation is the relatively low epoxide yield (9%), compared with α -pinene oxidation (34%).^[10] Another striking observation is that $[\text{alcohol}] + [\text{ketone}] \gg [\text{epoxide}]$, whereas during α -pinene oxidation, the amount of epoxide is equal to the amount of alcohol plus ketone (Figure 4). There-

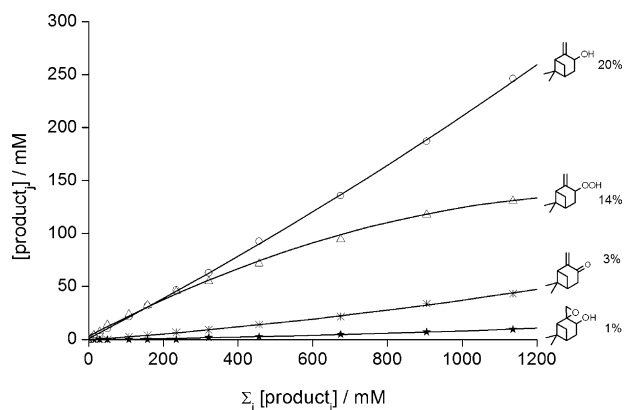


Figure 3. Evolution of the pinocarvyl products (b-site oxidation products in Scheme 1) versus the sum of the products. The selectivity is reported at 10% conversion (i.e., $\Sigma[\text{product}] = 630 \text{ mM}$).

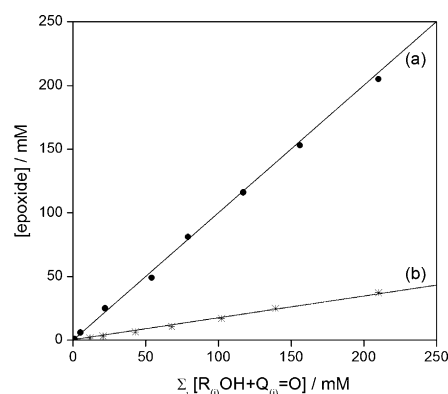


Figure 4. Correlation between the epoxide and the sum of alcohol and ketone concentrations during α - (a) and β -pinene (b) oxidation in the conversion range of 0–10%.

fore, it can be concluded that a different mechanism is responsible for the formation of alcohols and ketones.

Peroxy radical chemistry: Input from quantum chemical calculations

Numerical simulations of β -pinene oxidation show that the most abundant radicals in the system are peroxy radicals (see below). It is therefore instructive to investigate how these intermediates react with the substrate. For computational simplicity, a smaller model radical, namely, ethylperoxy, was used.

Abstraction of one of the two hydrogen atoms in the activated b position (Scheme 1, right) has slightly different barriers, that is, 10.7 and 13.0 kcal mol^{-1} , depending on the orientation of the hydrogen atoms towards the dimethyl bridge (UB3LYP/6-311++G(df,pd)//UB3LYP/6-31G(d,p) level of theory). The slightly lower barrier, in comparison with α -pinene (i.e., 12.5 kcal mol^{-1}), can be attributed to the 2.9 kcal mol^{-1} lower stability of the β -pinene isomer. Based on a typical pre-factor per hydrogen atom (i.e., $3.25 \times 10^8 \text{ M}^{-1} \text{ s}^{-1}$), one can thus estimate a rate constant for hydrogen abstraction of $k_{\text{abs}}(363 \text{ K}) \approx 120 \text{ M}^{-1} \text{ s}^{-1}$. The resonance-stabilised radical is shown on the

right-hand side in Scheme 2, together with the Mulliken atomic spin densities of the most relevant atoms. Addition of O₂ to this resonance-stabilised radical yields pinocarvyl peroxy (R_(b)-OO•) and myrtenyl peroxy (R_(d)-OO•) radicals. From the observed myrtenyl to pinocarvyl ratio of about 1.3, one can conclude that addition of O₂ to the d site is slightly favoured over the b site, which is in agreement with the slightly higher spin density at the d site C atom (see Scheme 2). Note that abstraction at the tertiary bridgehead position is strongly disfavoured, since that would lead to an sp² centre at the bridgehead. The calculated energy barrier is 17.6 kcal mol⁻¹, which is too high to be of any importance at moderate temperatures.

The barrier for the addition of a peroxy radical to the C=C double bond of β-pinene was computationally predicted to be 13.0 or 13.6 kcal mol⁻¹, depending on how the C=C bond was approached. Note that addition to the less-substituted end of the β-pinene double bond is favoured (the d site, Scheme 1), due to the higher stability of the resulting radical.^[21] Combining the predicted barriers with a typical pre-factor of 2 × 10⁸ M⁻¹ s⁻¹ (for example, determined for the addition of the methylperoxy radical to propylene^[22]) results in an addition rate constant, *k*_{addr}, of 4.3 M⁻¹ s⁻¹. Subsequent unimolecular release of an alkoxy radical and the corresponding epoxide is much faster and not rate determining (computed barrier of 7.0 kcal mol⁻¹).

The ratio of the predicted rate constant for hydrogen abstraction (120 M⁻¹ s⁻¹) over that for addition (4.3 M⁻¹ s⁻¹) is much larger for β-pinene than for α-pinene (16.6 versus 2.3); this explains the significantly lower epoxide yield observed for β-pinene.

The source of alcohol and ketone

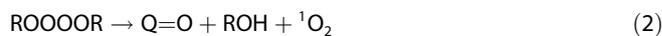
One remarkable difference between the oxidation of α- and β-pinene is that a large fraction of the peroxy radicals produced during β-pinene are primary peroxy radicals (e.g., R_(d)-OO•) rather than secondary ones. The cross-reaction between primary peroxy radicals is known to be significantly faster than for secondary peroxy radicals (6 × 10⁸ versus 4 × 10⁷ M⁻¹ s⁻¹).^[23] Given the typical radical concentrations during autoxidations of about 10⁻⁷ M, relative to hydrogen abstraction (120 M⁻¹ s⁻¹) and C=C addition (4.3 M⁻¹ s⁻¹), such mutual cross-reactions cannot be neglected. Therefore, this cross-reaction needs to be carefully evaluated.

When two peroxy radicals react, they initially form a short-lived tetroxide ROOOOR intermediate [Reaction (1)], which is stabilised by 16 kcal mol⁻¹.^[24]

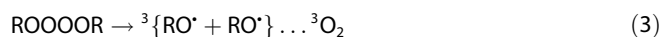


Ingold and Howard observed that tetroxides arising from primary and secondary peroxy radicals eliminated both singlet and triplet oxygen, whereas tetroxides arising from tertiary peroxy radicals eliminated only triplet oxygen.^[25] The structural influence on the singlet oxygen yield was confirmed by Mendenhall and Niu, who reported values of 0 (tertiary) and 4–13% (primary, secondary).^[26] Together with the observed kinetic isotope

effect,^[24] these findings provided strong experimental evidence for the Russell rearrangement^[27] of the tetroxide, leading to termination [Reaction (2)]. Recently, Peeters et al. proposed a mechanism to explain the formation of singlet oxygen, via a five-membered, cyclic transition state.^[28]

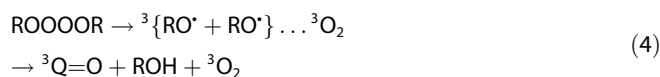


Not only is Reaction (2) possible, but scission of an O–O bond can also occur. According to Ghigo et al.,^[29] this leads to a loose complex, consisting of triplet oxygen and two alkoxy radicals [Reaction (3)]. Hasson et al. described the complex rather as alkoxy and trioxyl radicals, with ROOO• decaying into ³O₂ and RO•.^[30]



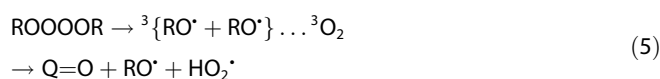
When considering the orientation of the two alkoxy radicals, they must have parallel spins, due to spin-conservation.^[31] Thus, they form a “spin-down” triplet opposite to the “spin-up” triplet of oxygen. Thermodynamic arguments prohibit the formation of singlet oxygen in that step (¹O₂ formation must be coupled to an exothermic reaction to be feasible).

Whether ³O₂ is loosely bound to the nascent alkoxy radical(s) from Reaction (3), or whether they are kept together by a solvent cage, has not yet been unambiguously proven, however, that does not qualitatively change the further outcome of the reaction. The fate of the nascent radicals can be threefold. Indeed, the first possibility is a mutual reaction between the two radicals, yielding electronically excited ketone [Reaction (4)]:

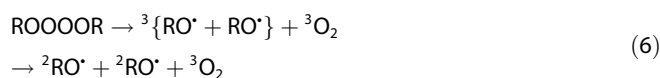


Notice that Reaction (4) leads to termination (i.e., a net decrease in radicals) and can, in principle, be monitored through the chemiluminescence of the excited ketone.^[32]

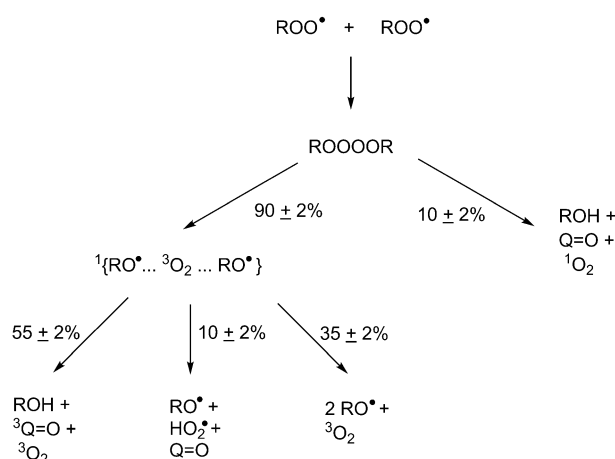
Alternatively, ³O₂ can react with one of the two RO• radicals, yielding ketone, RO• and HO₂• [Reaction (5)]:



Yet another possibility is the diffusive separation of the two radicals prior to a mutual reaction or reaction with ³O₂ [Reaction (6)].^[33]



Ab initio estimation of all involved branching fractions is currently prohibited and still an ongoing challenge for quantum chemistry.^[29,28,34] The branching fractions reported in Scheme 5 are the result of numerical simulation (see below) of the experimentally observed product distribution of β-pinene. The reported values are in agreement with the quantitative struc-



Scheme 5. Reaction channels in the cross-reactions of peroxy radicals.

ture–activity relationship (QSAR) suggested by Capouet et al. (i.e., $(50 \pm 20)\%$ non-terminating cross-reactions for primary peroxy radicals).^[35]

Interestingly, trace amounts of nopinone were detected in the product mixture. This is indeed a fingerprint for the occurrence of $^1\text{O}_2$, since the latter can, among other things, add to β -pinene to form a dioxetane that releases formaldehyde and nopinone.^[36] The Schenck $^1\text{O}_2$ addition product predominantly formed is indistinguishable from the autoxidation product $R_{(d)}\text{OOH}$.

Modelling shows that the cross-reaction of peroxy radicals is indeed the dominant source of alkoxy radicals during the autoxidation of β -pinene. These alkoxy radicals are converted into alcohols and ketones upon reaction with the substrate, the hydroperoxide and O_2 , respectively [Reactions (7)–(9)], analogous to the situation with α -pinene.



The formation of epoxide

Interestingly, epoxide selectivity increases from 5% at 1% conversion to approximately 10% at 20% conversion. This implies that, in addition to the primary epoxidation mechanism (analogous to the reactions shown in Scheme 3), there is also a secondary source of epoxide. Indeed, the addition of ROO^\bullet to β -pinene with subsequent epoxide formation is not fast enough to explain the observed bPO selectivity. As known from previous

work,^[10] the addition of aldehydes increases selectivity towards the epoxide. In the present case, an initial addition of 3 mol% myrtenal does indeed increase the epoxide selectivity from 6 to 9% at 2% conversion. This stems from the fact that the α -hydrogen atom of an aldehyde can be easily abstracted; the activation energy for abstraction was determined to be only 9 kcal mol^{-1} . With a typical pre-factor of $2 \times 10^8 \text{ M}^{-1} \text{ s}^{-1}$ for this bimolecular reaction, the rate constant becomes $763 \text{ M}^{-1} \text{ s}^{-1}$ at 363 K, that is, 6 times faster than hydrogen abstraction from β -pinene. This implies that for a hypothetical aldehyde yield of 14 mol%, an equal amount of peroxy radicals would react with the substrate and the aldehyde. Subsequently, the acyl radical will be converted into an acyl peroxy radical upon O_2 addition. Such acyl peroxy radicals can directly epoxidise $\text{C}=\text{C}$ bonds, similar to other peroxy radicals, much faster (namely, rate-determining addition barrier only $2.5 \text{ kcal mol}^{-1}$).^[37] Alternatively, the acyl peroxy radical can abstract an allylic hydrogen atom from the substrate and yield a peracid (computed barrier of 3 kcal mol^{-1}).^[38] Such peracids are known epoxidation agents, too (so-called Prilezhaev mechanism).^[39] Both channels thus lead to a secondary contribution to the bPO yield (see Scheme 6).

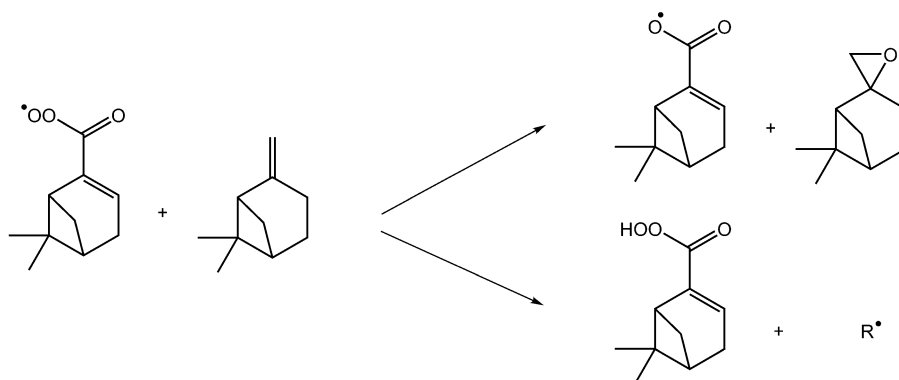
According to this mechanism, sizeable amounts of myrtenic acid and peracid are formed, which is in agreement with the experimental observations that 1) there is a small myrtenic acid peak in the chromatogram and 2) this peak increases by about 20% upon reduction of the sample with phosphine.

HO_2^\bullet chemistry

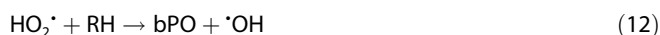
Considerable amounts of HO_2^\bullet radicals are produced during the autoxidation of β -pinene, for instance, in Reactions (5) and (9). These HO_2^\bullet radicals equilibrate with ROO^\bullet radicals, according to Reaction (10). The forward and reverse rate constants for Reaction (10) can be estimated to be 1.8×10^4 and $3 \times 10^3 \text{ M}^{-1} \text{ s}^{-1}$, respectively.^[40]



Alternatively, HO_2^\bullet can also abstract hydrogen atoms from the substrate [Reaction (11)], or add to the $\text{C}=\text{C}$ bond of the substrate and yield an epoxide [Reaction (12)].



Scheme 6. Co-oxidation of myrtenal and the secondary contribution to the epoxide formation.



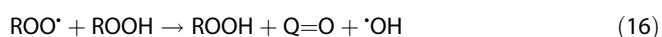
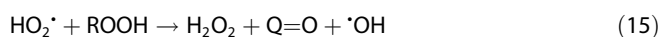
However, HO_2^{\cdot} radicals also play a role in determining the overall radical concentration because they can terminate in a diffusion-controlled manner, according to Reactions (13) and (14).^[41,42]



Modelling shows that the H_2O_2 concentration steadily grows up to 6 mM at 20% conversion, that is, low and difficult to quantify in the complex reaction mixture.

Over-oxidation of the hydroperoxides

Myrtenyl and pinocarvyl hydroperoxides have weakly bonded α -hydrogen atoms that can be abstracted by peroxy and hydroperoxy radicals, yielding additional ketone [Reactions (15) and (16)].^[43]



In principle, the $\text{}^{\cdot}\text{OH}$ radical released in this step can trigger an activated cage reaction, producing some additional alcohol.^[44] However, for activated substrates, such as ethylbenzene^[17] and α -pinene,^[10,11] and hence, also β -pinene, the importance of this alcohol production channel can be neglected in first approximation.

Chain initiation

It was found that during the autoxidation of cyclohexane radicals were formed in the bimolecular reaction of cyclohexyl hydroperoxide and cyclohexanone.^[18] In this reaction, the OH radical, breaking away from the hydroperoxide, abstracts a weakly bonded α -hydrogen atom from the ketone, producing a resonance-stabilised ketonyl radical, water and an alkoxyl radical. A similar initiation should take place in the autoxidation of β -pinene, since a resonance-stabilised allyl radical can be formed [Reaction (17)].



The barrier of the analogous reaction between propene and methyl hydroperoxide was computationally predicted to be $22.7 \text{ kcal mol}^{-1}$ at the CBS-QB3 level of theory. This value can be isodesmically extrapolated to β -pinene, based on the difference in the DFT barrier of $6.9 \text{ kcal mol}^{-1}$ between β -pinene and propene (UB3LYP/6-311++G(df,pd)//UB3LYP/6-31G(d,p) level of theory). However, the transition state of Reaction (17) should be considered as a singlet diradical. Although an advanced level of theory, CBS-QB3 systematically overestimates the energy in the computation of open-shell singlets by $(5.8 \pm$

$0.5) \text{ kcal mol}^{-1}$.^[45] Also taking this effect into consideration, one can estimate an initiation barrier of $(22 \pm 3) \text{ kcal mol}^{-1}$, that is, significantly lower than in the case of cyclohexanone $((27 \pm 1) \text{ kcal mol}^{-1})$.^[18] This result confirms the higher efficiency of the bimolecular initiation mechanism over the unimolecular decomposition mechanism: the latter facing a barrier of roughly 40 kcal mol^{-1} (homolytic hydroperoxide cleavage). In principle, since the substrate is an olefin, OH transfer from ROOH to the double bond (instead of H transfer from the substrate to ROOH) needs to be considered as an alternative initiation mechanism. However, evaluating such a reaction on the structure- and spin-contamination-corrected CBS-QB3 level, the corresponding barrier amounts to $(28 \pm 3) \text{ kcal mol}^{-1}$, such that OH transfer can have only a minor influence on the total initiation at moderate temperatures, as encountered in this study.

Unfortunately, bimolecular initiation is very demanding to describe from a computational point of view because spin and dynamic effects will play an important role. For instance, intrinsic reaction coordinate (IRC) analysis of the reaction suggests that the located transition state would connect not only to alkoxyl, water and allyl, but further on to two closed-shell alcohol products. However, IRC analysis follows the energetically steepest descent path, but neglects entropic effects, as well as potential solvent (cage) effects. More work is required to computationally describe this reaction in detail, preferably by using multi-reference methods to accurately describe state mixing.^[46]

Kinetic modelling

A kinetic model was set up in Matlab by using the ODE15s solver for stiff ordinary differential equations (ODEs). The initial conditions for solving the ODEs were obtained from experimental data. Initial estimations of the rate constants were determined either from quantum chemical predictions or from known rate constants reported in the literature. To reduce the complexity, and due to limited available kinetic data, regioisomeric products were lumped together, similar to a recent study on atmospheric limonene oxidation.^[47] This assumption implies that both radical sites in the R^{\cdot} radical are equivalent and means, for instance, that ROH stands for myrtenol plus pinocarveol. Note that this also implies that the myrtenyl and pinocarvyl peroxy radicals are assumed to react similarly. Although this is a good approximation for hydrogen abstraction and C=C addition, it might be too simplified for the peroxy cross-reactions. On the other hand, this is an elegant way of keeping the complexity under control, while, at the same time, (approximately) taking into account the effect of cross-reactions between $\text{R}_{(\text{b})}\text{-OO}^{\cdot}$ and $\text{R}_{(\text{d})}\text{-OO}^{\cdot}$ radicals.^[35] Table 1 summarises the different reactions taken into account, together with the corresponding rate constants.

Based on this model, the evolution of hydroperoxides, epoxide, alcohols and ketones can be described rather accurately (see Figures 5 and 6). The small deviations ($< 30\%$) are probably due to simplifications made in the model, as well as experimental errors.

Interesting numbers that can be extracted from this modelling are, for instance, radical concentrations, for example,

Table 1. Overview of the different reactions implemented in the kinetic modelling, together with the corresponding rate constants.

Reaction	k kinetic model [$M^{-1}s^{-1}$]	Reference reaction	k reference [$M^{-1}s^{-1}$]	Ref.
$ROOH + RH \rightarrow RO^{\cdot} + H_2O + R^{\cdot}$	1.6×10^{-5}	see text	1.7×10^{-5}	[48]
$ROO^{\cdot} + RH \rightarrow ROOH + R^{\cdot}$	80	$CH_3CH_2OO^{\cdot} + bP$	120	[48]
$RO^{\cdot} + RH \rightarrow ROH + R^{(a)}$	5.0×10^6	α -pinene substrate	5.0×10^6	[10]
$RO^{\cdot} + ROOH \rightarrow ROH + ROO^{(a)}$	1.5×10^{10}	$tBuO^{\cdot} + tBuOOH$	1.5×10^{10}	[49]
$OH^{\cdot} + RH \rightarrow H_2O + R^{(a)}$	2×10^9	$(C_2H_5)_2C=CH_2 + OH^{\cdot}$	2×10^9	[50]
$HO_2^{\cdot} + RH \rightarrow H_2O + R^{(a)}$	7.6	$HO_2^{\cdot} + bP$	7.6	[51]
$O_2 + R^{\cdot} \rightarrow ROO^{(a)}$	2.0×10^9	diffusion controlled	2.0×10^9	
$RO^{\cdot} + O_2 \rightarrow Q=O + HO_2^{(a)}$	1.2×10^7	$O_2 + n-C_4H_9O^{\cdot}$	1.2×10^7	[52]
$ROO^{\cdot} + ROOH \rightarrow ROOH + Q=O + ^{\cdot}OH$	128	$EtOO^{\cdot} + R_{(b)}-OOH$	126	[48]
$ROO^{\cdot} + Q_{(d)}=O \rightarrow ROOH + Q'_{(d)}=O$	572	$EtOO^{\cdot} + Q_{(d)}=O$	763	[48]
$HO_2^{\cdot} + ROOH \rightarrow H_2O_2 + ROO^{(a)}$	1.8×10^4	$HO_2^{\cdot} + CH_3OOH$	1.8×10^4	[48]
$ROO^{\cdot} + H_2O_2 \rightarrow ROOH + HO_2^{(a)}$	3×10^3	$CH_3OO^{\cdot} + H_2O_2$	3×10^3	[48]
$ROO^{\cdot} + RH \rightarrow bPO + RO^{\cdot}$	6	$EtOO^{\cdot} + bP \rightarrow bPO + EtO^{\cdot}$	4.3	[48]
$HO_2^{\cdot} + RH \rightarrow bPO + HO^{(a)}$	17	$CH_3CH=CH_2 + HO_2^{\cdot}$	17	[51]
$2ROO^{\cdot} \rightarrow \text{termination} + \text{propagation}$	3.9×10^8	$2n-C_4H_9O_2^{\cdot}$	6×10^8	[23]
$2HO_2^{\cdot} \rightarrow H_2O_2 + O_2^{(a)}$	1.3×10^9	$2HO_2^{\cdot}$	1.3×10^9	[48]
$HO_2^{\cdot} + ROO^{\cdot} \rightarrow O_2 + ROOH$	8.8×10^9	$HO_2^{\cdot} + n-C_4H_9O_2^{\cdot}$	9.8×10^9	[41]

[a] Reactions with low sensitivity (perturbation of the rate constants with 20% did not induce a significant change in the product–time curves, and hence could, not be optimised with the experimental data; for these reactions the reference values were used).

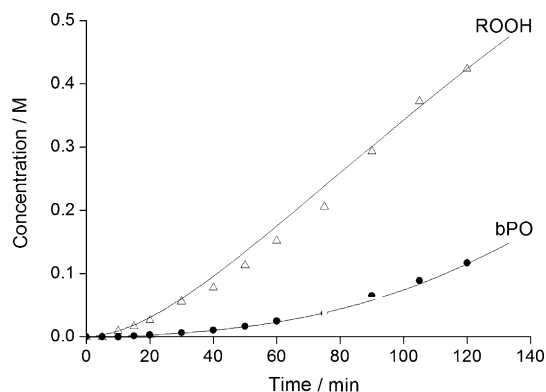


Figure 5. Evolution of the hydroperoxides (i.e., $R_{(b)}-OOH$ plus $R_{(d)}-OOH$) and β -pinene oxide (bPO) as a function of time; solid line is the result of a numerical simulation (see text).

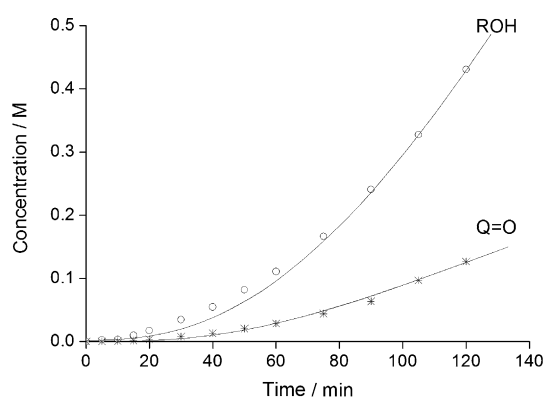


Figure 6. Evolution of the alcohols (i.e., $R_{(b)}-OH$ plus $R_{(d)}-OH$) and the carbonyl compounds (i.e., $Q_{(b)}=O$ plus $Q_{(d)}=O$) as a function of time; solid line is the result of a numerical simulation (see text).

$[ROO^{\cdot}] = 3 \times 10^{-7} M$ and $[RO^{\cdot}] = 1.5 \times 10^{-14} M$ at 10% conversion. It also shows that hydrogen abstraction from β -pinene ($1.5 \times 10^{-4} M s^{-1}$) and the bimolecular peroxy cross-reaction ($8.0 \times 10^{-5} M s^{-1}$) are both important ROO^{\cdot} channels, leading to products. Initiation Reaction (17) and the ROO^{\cdot} cross-reactions, summarised in Scheme 5, are the most important RO^{\cdot} sources; epoxidation of β -pinene, according to the mechanism in Scheme 3, is only a minor source of RO^{\cdot} radicals. More results from the modelling study can be found in the Supporting Information.

Chain length

The chain length, ν (i.e., the ratio of the rate of chain propagation and the rate of chain termination), is given by Equation (1); $k_{\text{non-term}}$ and k_{term} refer to the rate constants of the non-terminating and terminating cross-reactions, respectively, of the combined peroxy radicals. Figure 7 shows the evolution of ν as a function of conversion.

$$\nu = \frac{R_{\text{prop}}}{R_{\text{term}}} = \frac{(k_{\text{abs}} + k_{\text{add}})[ROO^{\cdot}][RH] + k_{\text{non-term}}[ROO^{\cdot}]^2}{k_{\text{term}}[ROO^{\cdot}]^2} \quad (1)$$

The ratio of mono- over biradical propagation reactions in Figure 7 shows that peroxy hydrogen abstractions and additions are only responsible for the formation of 60% of products.

Temperature dependence

The effect of the temperature on the reaction rate at 2% conversion is summarised in the Arrhenius plot given in Figure 8.

The experimentally observed activation energy is $(21 \pm 2) \text{ kcal mol}^{-1}$ and the Arrhenius pre-factor is $3 \times 10^8 \text{ M}^{-1} \text{ s}^{-1}$. Based on quasi-steady-state analysis, it can be shown that the experimentally observed activation energy equals $E_{\text{prop}} + (E_{\text{init}}/$

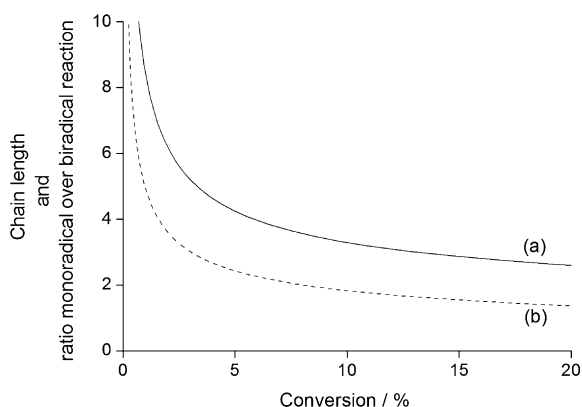


Figure 7. Evolution of chain length ν (a) and the ratio of mono- over biradical propagation reactions (b) as a function of the β -pinene conversion.

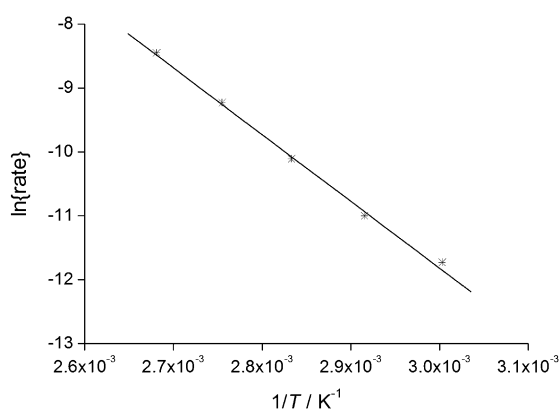


Figure 8. Arrhenius plot of the uncatalysed β -pinene autoxidation. The logarithm of the reaction rate at 2% conversion is shown for 333, 343, 353, 363 and 373 K (correlation coefficient = 0.997).

$2) - (E_{\text{cross}}/2)$.^[53] The barrier of the radical cross-reaction can be assumed to be very small ($E_{\text{cross}} \leq 2 \text{ kcal mol}^{-1}$). The relevant propagation barrier is the thermally averaged barrier for hydrogen abstraction and peroxy radical addition ($E_{\text{prop}} \approx 11 \text{ kcal mol}^{-1}$). The initiation barrier [namely, Reaction (17)] was estimated to be 22 kcal mol^{-1} (see above). Putting all these values together, one expects, according to the proposed mechanism, an apparent activation energy of $(21 \pm 4) \text{ kcal mol}^{-1}$, which is in excellent agreement with experimental results.

Conclusion

The radical chain autoxidation of β -pinene was compared with previous results for the isomer α -pinene. Resonance-stabilised alkyl radicals were generated upon abstraction of an allylic hydrogen atom. Addition of O_2 to these R^{\bullet} radicals yielded myrtenyl and pinocarvyl peroxy radicals. These radicals did not only abstract hydrogen atoms, regenerating the alkyl radicals, but also added to the $\text{C}=\text{C}$ double bond; a reaction that ultimately led to epoxide and alkoxy radicals. Another reaction of

the peroxy radicals, which was much more important for β -pinene than for α -pinene, was the cross-reaction of two peroxy radicals. Numerical simulation of the reaction revealed that approximately 60% of the cross-reactions led to chain termination, compensating for the chain-initiation reaction between a hydroperoxide product and the RH substrate. However, 40% of the peroxy cross-reactions did not lead to the destruction of radicals and actually contributed to chain propagation. Hence, β -pinene oxidation was characterised by mono- and biradical chain propagations; the ratio between these channels was approximately 2:1 at 10% conversion. This behaviour deviated from that of cyclohexane, for which the reaction was dominated by monoradical propagations.^[16] The importance of these biradical cross-reactions is not only clear from modelling, but also from the formation of nopinone, which is a product that is an indicator of singlet oxygen, produced in a small fraction (i.e., 10%) in the cross-reaction of the peroxy radicals. Alkoxy radical concentrations increased were about 10^{-14} M and were predominantly formed in the biradical cross-reactions of peroxy radicals. RO^{\bullet} radicals are the precursors of the observed alcohols and carbonyl products. Co-oxidation of myrtenal, which is a primary aldehyde product, causes the formation of additional β -pinene oxide.

Experimental Section

The experiments were performed in a glass 10 mL bubble column reactor equipped with a condenser. O_2 was bubbled (100 NmL min^{-1}) through 250 μm pores of a bubbler to ensure fast gas-liquid mass transfer. The temperature was controlled by a thermostat, equipped with an immersion heater and thermocouple (standard run at $(363 \pm 2) \text{ K}$). The reactor was heated to the reaction temperature under a flow of N_2 (inert conditions); subsequently the gas flow was changed to O_2 to start the reaction. **Caution!** This is potentially dangerous and appropriate safety measures should be taken. Samples ($\pm 250 \mu\text{L}$ each) were withdrawn from the reactor and analysed by GC (HP6890; HP-5 column, 30 m/0.32 mm/0.25 μm ; flame ionization detector). *n*-Nonane (Sigma Aldrich, > 99%) was added to the ($-$)- β -pinene substrate (Sigma Aldrich, 99%) and used as an inert internal standard (1 mol%). The hydroperoxide yields were determined by double injection, with and without reduction of the reaction mixture by trimethylphosphine (Sigma Aldrich, 1 M in toluene). From the obtained augmentation in alcohol content, the corresponding hydroperoxide yield was determined. Products were identified by GC-MS, using split injection ($T_{\text{inject}} = 250^\circ\text{C}$) and cool-on-column injection ($T_{\text{inject}} = 50^\circ\text{C}$), to verify the thermal stability of the products. No difference in product distribution could be observed. Products were additionally characterised by their Kovats indices (see the Supporting Information).

Quantum chemical calculations were performed with Gaussian 09 software^[54] at the UB3LYP/6-311 + G(df,pd)//UB3LYP/6-31G(d,p) level of theory.^[55] Earlier, this method was validated against several benchmark levels of theory (namely, G2M, G3 and CBS-QB3) for hydrogen-abstraction reactions by peroxy radicals.^[16] The reported relative energies of the stationary points on the potential energy surfaces (namely, the energy barriers E_b and reaction energies ΔE) were corrected for zero-point energy (ZPE) differences.

Acknowledgements

Financial support of the ETH Zurich is kindly acknowledged. E.M. is grateful for the Schweizerische Gesellschaft der Verfahrens- und ChemieingenieurInnen Thesis Award 2011.

Keywords: autoxidation • kinetics • radical reactions • renewable resources • singlet oxygen

- [1] M. Gscheidmeier, H. Fleig, *Turpentine*, in *Ullmann's Encyclopedia of Industrial Chemistry*, Wiley-VCH, Weinheim, **2005**.
- [2] *Pulp and Paper Capacities*, Food and Agriculture Organisation of the United Nations, Rome, **2008**.
- [3] R. Rinaldi, F. Schüth, *ChemSusChem* **2009**, *2*, 1096.
- [4] K. G. Fahlbusch, F. J. Hammerschmidt, J. Panten, W. Pickenhaben, D. Schatkowski, *Flavors and Fragrances*, in *Ullmann's Encyclopedia of Industrial Chemistry*, Wiley-VCH, Weinheim, **2005**.
- [5] J. P. Vité, W. Francke, *Chem. Unserer Zeit* **1985**, *19*, 11.
- [6] K. Bauer, D. Garbe, H. Surburg, *Common Fragrance and Flavour Materials*, Wiley-VCH, Weinheim, **1997**.
- [7] D. V. Banthorpe, D. Whittaker, *Chem. Rev.* **1966**, *66*, 643.
- [8] A. Mosandl, U. Hener, P. Kreis, H.-G. Schmarr, *Flavour Fragrance J.* **1990**, *5*, 193.
- [9] G. Widmark, S.-G. Blohm, *Acta Chem. Scand.* **1957**, *11*, 392.
- [10] U. Neuenschwander, F. Guignard, I. Hermans, *ChemSusChem* **2010**, *3*, 75.
- [11] U. Neuenschwander, I. Hermans, *Phys. Chem. Chem. Phys.* **2010**, *12*, 10542.
- [12] M. J. da Silva, P. Robles-Dutenhefner, L. Menini, E. V. Gusevskaya, *J. Mol. Catal. A: Chem.* **2003**, *201*, 71.
- [13] C. C. Guo, W. J. Yang, Y. L. Mao, *J. Mol. Catal. A: Chem.* **2005**, *226*, 279.
- [14] E. F. Murphy, T. Mallat, A. Baiker, *Catal. Today* **2000**, *57*, 115.
- [15] P. A. Robles-Dutenhefner, M. J. da Silva, L. S. Sales, E. M. B. Sousa, E. V. Gusevskaya, *J. Mol. Catal. A: Chem.* **2004**, *217*, 139.
- [16] I. Hermans, T. L. Nguyen, P. A. Jacobs, J. Peeters, *ChemPhysChem* **2005**, *6*, 637.
- [17] I. Hermans, J. Peeters, P. Jacobs, *J. Org. Chem.* **2007**, *72*, 3057.
- [18] I. Hermans, P. A. Jacobs, J. Peeters, *Chem. Eur. J.* **2006**, *12*, 4229.
- [19] Q. Wang, S. Y. Fan, H. N. C. Wang, Z. Li, B. M. Fung, R. J. Twieg, H. T. Nguyen, *Tetrahedron* **1993**, *49*, 619.
- [20] Although the ol-epoxide by-products could, in principle, also be formed through a unimolecular rearrangement of the peroxy radicals; this would imply that the compounds would be primary in origin (see the Supporting Information).
- [21] The resulting radical is tertiary and benefits from hyperconjugation of the cyclobutyl group. For unactivated olefins, such as propene, opposite selectivities have been computationally postulated: C. C. Chen, J. W. Bozzelli, *J. Phys. Chem. A* **2000**, *104*, 4997. However, it would be difficult to verify experimentally that claim, since the formed intermediate quickly rearranges into epoxide.
- [22] W. Tsang, *J. Phys. Chem. Ref. Data* **1991**, *20*, 221.
- [23] B. G. Glover, T. A. Miller, *J. Phys. Chem. A* **2005**, *109*, 11191.
- [24] P. A. Denis, F. R. Ornellas, *J. Phys. Chem. A* **2009**, *113*, 499.
- [25] J. A. Howard, K. U. Ingold, *J. Am. Chem. Soc.* **1968**, *90*, 1056.
- [26] Q. J. Niu, G. D. Mendenhall, *J. Am. Chem. Soc.* **1992**, *114*, 165.
- [27] D. J. Bogan, J. J. Havel, R. A. Coveleskie, F. Celii, B. J. Stammerjohn, W. A. Sanders, F. W. Williams, H. W. Carhart, *Symp. Int. Comb.* **1981**, *18*, 843.
- [28] T. L. Nguyen, L. Vereecken, J. Peeters, *Z. Phys. Chem.* **2010**, *224*, 1081.
- [29] G. Ghigo, A. Maranzana, G. Tonachini, *J. Chem. Phys.* **2003**, *118*, 10575.
- [30] A. S. Hasson, K. T. Kuwata, M. C. Arroyo, E. B. Petersen, *J. Photochem. Photobiol. A* **2005**, *176*, 218.
- [31] E. P. Wigner, *Proc. Natl. Acad. Sci. USA* **1964**, *51*, 956.
- [32] C. A. Tolman, J. D. Druliner, M. J. Nappa, N. Herron in *Activation and Functionalization of Alkanes*, (Ed.: C. L. Hill), Wiley-VCH, Weinheim, **1989**.
- [33] P. D. Lightfoot, R. A. Cox, J. N. Crowley, M. Destriau, G. D. Hayman, M. E. Jenkin, G. K. Moortgat, F. Zabel, *Atmos. Environ.* **1992**, *27A*, 1805.
- [34] T. S. Dibble, *Atmos. Environ.* **2008**, *42*, 5837.
- [35] M. Capouet, J. Peeters, B. Nozière, J.-F. Müller, *Atmos. Chem. Phys.* **2004**, *4*, 2285.
- [36] D. R. Kearns, *Chem. Rev.* **1971**, *71*, 395.
- [37] Experimental values for similar substrates range from 4 to 6 kcal mol⁻¹, see: R. R. Diaz, K. Selby, D. J. Waddington, *J. Chem. Soc. Perkin Trans. 2* **1977**, 360.
- [38] The subsequent destructive cage reaction (peracid + allyl radical, giving acyloxy radical and alcohol) faces an activation energy of 9.9 kcal mol⁻¹. In comparison with the unactivated cage reaction in cyclohexane autoxidation (CyOOH + alkyl radical, giving alkoxy radical and alcohol), for which the barrier is 6.8 kcal mol⁻¹ and the cage efficiency is 5%,^[16] one can exclude the contribution of such a cage reaction in the present case.
- [39] N. Prileschajew, *Ber. Dtsch. Chem. Ges.* **1909**, *42*, 4811.
- [40] W. Tsang, R. F. Hampson, *J. Phys. Chem. Ref. Data* **1986**, *15*, 1087.
- [41] J. Thiebaud, C. Fittschen, *Appl. Phys. B* **2006**, *85*, 383.
- [42] D. Johnson, D. W. Price, G. Marston, *Atmos. Environ.* **2004**, *38*, 1447.
- [43] L. Vereecken, T. L. Nguyen, I. Hermans, J. Peeters, *Chem. Phys. Lett.* **2004**, *393*, 432.
- [44] I. Hermans, J. Peeters, P. A. Jacobs, *Top. Catal.* **2008**, *50*, 124.
- [45] B. Sirjean, R. Fournet, P.-A. Glaude, M. F. Ruiz-López, *Chem. Phys. Lett.* **2007**, *435*, 152.
- [46] T. Saito, S. Nishihara, S. Yamanaka, Y. Kitagawa, T. Kawakami, S. Yamada, H. Isobe, M. Okumura, K. Yamaguchi, *Theor. Chem. Acc.* **2011**. DOI: 10.1007/s00214-011-0914-z.
- [47] C. Rio, P.-M. Flaud, J.-C. Loison, E. Villenave, *ChemPhysChem* **2010**, *11*, 3962.
- [48] The energy barrier was obtained from quantum chemical calculation, based on UB3LYP/6-311 + + G(df,pd)/UB3LYP/6-31G(d,p) density functional theory, including a ZPE correction.
- [49] N. Turrà, U. Neuenschwander, A. Baiker, J. Peeters, I. Hermans, *Chem. Eur. J.* **2010**, *16*, 13226.
- [50] D. Grosjean, E. L. Williams, *Atmos. Environ. Part A* **1992**, *26*, 1395.
- [51] The literature values from reference [21] for abstraction and addition of HOO• to propene (i.e., 0.18 and 2.8 m⁻¹ s⁻¹, respectively) were corrected by DFT-based energy increments of 2.7 and 1.3 kcal mol⁻¹, respectively, yielding values of 7.6 and 17 m⁻¹ s⁻¹, respectively, at 363 K.
- [52] R. Atkinson, D. L. Baulch, R. A. Cox, J. N. Crowley, R. F. Hampson, R. G. Hynes, M. E. Jenkin, M. J. Rossi, J. Troe, *Atmos. Chem. Phys.* **2006**, *6*, 3625.
- [53] This expression stems from the differential d[ln(r)]/d(1/T), applied to the rate equation $r(T) = k_{prop}(T) [ROO]_{oss}(T) [RH]$, neglecting the temperature dependency of the biradical cross-reactions.
- [54] Gaussian 09, Revision A.02, M. J. Frisch, G. W. Trucks, H. B. Schlegel, G. E. Scuseria, M. A. Robb, J. R. Cheeseman, J. A. Montgomery, Jr., T. Vreven, K. N. Kudin, J. C. Burant, J. M. Millam, S. S. Iyengar, J. Tomasi, V. Barone, B. Mennucci, M. Cossi, G. Scalmani, N. Rega, G. A. Petersson, H. Nakatsuji, M. Hada, M. Ehara, K. Toyota, R. Fukuda, J. Hasegawa, M. Ishida, T. Nakajima, Y. Honda, O. Kitao, H. Nakai, M. Klene, X. Li, J. E. Knox, H. P. Hratchian, J. B. Cross, V. Bakken, C. Adamo, J. Jaramillo, R. Gomperts, R. E. Stratmann, O. Yazyev, A. J. Austin, R. Cammi, C. Pomelli, J. W. Ochterski, P. Y. Ayala, K. Morokuma, G. A. Voth, P. Salvador, J. J. Dannenberg, V. G. Zakrzewski, S. Dapprich, A. D. Daniels, M. C. Strain, O. Farkas, D. K. Malick, A. D. Rabuck, K. Raghavachari, J. B. Foresman, J. V. Ortiz, Q. Cui, A. G. Baboul, S. Clifford, J. Cioslowski, B. B. Stefanov, G. Liu, A. Liashenko, P. Piskorz, I. Komaromi, R. L. Martin, D. J. Fox, T. Keith, M. A. Al-Laham, C. Y. Peng, A. Nanayakkara, M. Challacombe, P. M. W. Gill, B. Johnson, W. Chen, M. W. Wong, C. Gonzalez, J. A. Pople, Gaussian, Inc., Wallingford CT, **2009**.
- [55] a) A. D. Becke, *J. Chem. Phys.* **1992**, *96*, 2155; b) A. D. Becke, *J. Chem. Phys.* **1992**, *97*, 9173; c) A. D. Becke, *J. Chem. Phys.* **1993**, *98*, 5648; d) C. Lee, W. Yang, R. G. Parr, *Phys. Rev. B* **1988**, *37*, 785.

Received: May 25, 2011

Published online on September 7, 2011